is simply to bring the four carboxylic pendant arms on the same side of the ring.

The conformational preference of the 14-membered macrocycles also has a direct influence on the choice of the coordination polyhedron of the lanthanide ion. Indeed, the four heteroatoms of the conformations reproduced in Figure 3 are not coplanar, two of them being higher and two of them being lower than their mean plane. Only a dodecahedal structure could fit such an arrangement. Prior to the present crystallographic analysis, we could thus have proposed a geometrical model of TbTETA in the solid just as the structures of the DOTA complexes were easily foreseen because their was only one reasonable expectation.[5,6]

Packing Pattern. The packing pattern of Na^+ [TbTETA]$^-$·$6H_2O$·$^1/_2$NaCl is rather unusual (see Figure 4; packing interatomic distances and corresponding angles are available as supplementary material). The crystal consists of layers parallel to the *b*,*c* plane. These layers succeed each other at intervals of half the length of the unit cell along *a*; in addition to water molecules, they contain alternatively Na^+[TbTETA]$^-$ units or chloride ions. Within the layers located at around $x = 0.5$ (Figure 4A), TbTETA complex units are held together via water molecules and sodium ions that form with the TETA carboxylate oxygens a mixed network of O···O and Na···O close contacts. The Na···O and O···O contacts (probable hydrogen bonds) range from 2.320 (4) to 2.533 (3) Å and from 2.826 (4) to 2.869 (6) Å, respectively. It should be noted that particularly large amplitudes of thermal vibration are observed for the sodium ions Na(2) (rms values varying between 0.195 and 0.446 Å) and for the two water oxygens O(w7) (rms amplitudes between 0.255 and 0.346 Å) and O(w2) (rms amplitudes between 0.205 and 0.508 Å). Within the aqueous layers, which are located at around $x = 0$, the chloride ions and four symmetrically independant water molecules form an interesting network of hydrogen bonds, based on four- and five-membered rings. The corresponding pattern is shown in Figure 4B. The five-membered puckered rings of water molecules extend in infinite chains, parallel to the *c* axis, by sharing either one oxygen atom or one ring edge (the O···O contacts range from 2.851 (6) to 2.984 (6) Å). Moreover, the chains are cross-linked via hydrogen bonds to chloride ions so that parallel chains of four-membered planar rings are generated along the *b* axis. The dihedral angle between two successive four-membered rings has a value of 66.9 (1)°. Finally, the coordination polyhedron of the chloride ions is a distorted tetrahedron (see supplementary material).

Acknowledgment. J.F.D. acknowledges the Fonds National de la Recherche Scientifique of Belgium for financial support. J.F.D. is Chercheur Qualifié at this institution.

Registry No. Na^+[TbTETA]$^-$·$6H_2O$·$^1/_2$NaCl, 92671-58-4.

Supplementary Material Available: Listings of observed and calculated structure factor amplitudes, anisotropic thermal parameters, hydrogen atom coordinates, and packing bond distances and corresponding angles (Tables SI–SIV) (22 pages). Ordering information is given on any current masthead page.

Contribution from the Institut für Physikalische und Theoretische Chemie der Universität Tübingen, 7400 Tübingen, West Germany, and Rocketdyne, A Division of Rockwell International Corporation, Canoga Park, California 91304

Gas-Phase Structure of Azidotrifluoromethane. An Electron Diffraction, Microwave Spectroscopy, and Normal-Coordinate Analysis

KARL O. CHRISTE,*[1a] DINES CHRISTEN,[1b] HEINZ OBERHAMMER,*[1b] and CARL J. SCHACK[1a]

Received February 28, 1984

The geometric structure of azidotrifluoromethane has been obtained by a combined analysis of electron diffraction intensities and ground-state rotational constants derived from the microwave spectrum. The following parameters were obtained (r_{av} values in Å and deg with 2σ uncertainties in units of the last decimal): C–F = 1.328 (2), C–N_α = 1.425 (5), N_α–N_β = 1.252 (5), N_β–N_ω = 1.118 (3), $\angle CN_\alpha N_\beta$ = 112.4 (2), $\angle N_\alpha N_\beta N_\omega$ = 169.6 (3.4), $\angle$FCF = 108.7 (2). The CF_3 group is in the staggered position with respect to the N_3 group and tilted away from it by 5.8 (4)°.

Introduction

Structural data on covalent azides are rare due to the explosive nature[2,3] and handling difficulties encountered with these compounds. One of the more stable covalent azides is CF_3N_3, a compound originally prepared by Makarov and co-workers[4,5] and recently studied in more detail by two of us.[6] Although the closely related CH_3N_3 molecule has previously been studied by both electron diffraction[7] and microwave spectroscopy,[8] the available data were insufficient to determine whether the N_3 group is linear and to obtain a reliable value for the tilt angle of the methyl group. Furthermore, a comparison of the structures of CH_3N_3 and CF_3N_3 was expected to contribute to our knowledge of how the substitution of a CH_3 group by a CF_3 group influences the structure of the rest of the molecule.[9]

Experimental Section

Synthesis and Handling of CF_3N_3. The sample of CF_3N_3 was prepared as previously described.[6] Prior to the electron diffraction experiments, a small amount of N_2 formed by decomposition of some CF_3N_3 was pumped off at −196 °C. The only other decomposition

(1) (a) Rocketdyne. (b) University of Tübingen.
(2) Patai, S., Ed.; "The Chemistry of the Azido Group"; Wiley-Interscience: New York, 1971.
(3) Dehnicke, K. *Adv. Inorg. Chem. Radiochem.* **1983**, *26*, 169.
(4) Makarov, S. P.; Yakubovich, A. Ya.; Ginsburg, V. A.; Filatov, A. S.; Englin, M. A.; Privezentseva, N. F.; Nikiforova, T. Ya. *Dokl. Akad. Nauk SSSR* **1961**, *141*, 357.
(5) Makarov, S. P.; Yakubovich, A. Ya.; Filatov, A. S.; Englin, M. A.; Nikiforova, T. Ya. *Zh. Obshch. Khim.* **1968**, *38*, 709.
(6) Christe, K. O.; Schack, C. J. *Inorg. Chem.* **1981**, *20*, 2566.
(7) (a) Livingston, R. L.; Rao, C. N. R. *J. Phys. Chem.* **1960**, *64*, 756. (b) Anderson, D. W. W.; Rankin, D. W. H.; Robertson, A. *J. Mol. Struct.* **1972**, *14*, 385.
(8) Salathiel, W. M.; Curl, R. F., Jr. *J. Chem. Phys.* **1966**, *44*, 1288.
(9) Oberhammer, H. *J. Fluorine Chem.* **1983**, *23*, 147.

0020-1669/84/1323-4283$01.50/0

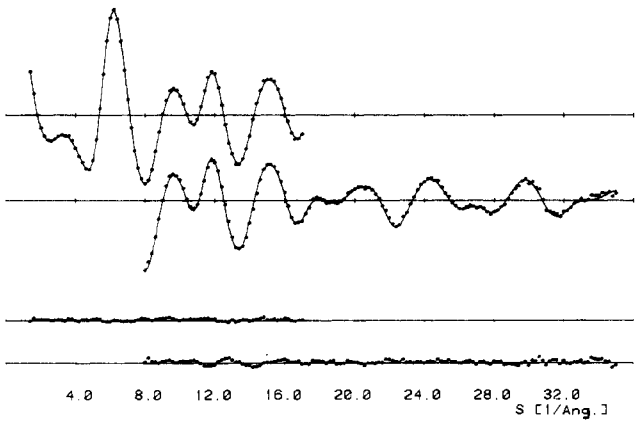

Figure 1. Experimental (···) and calculated (—) molecular intensities and differences.

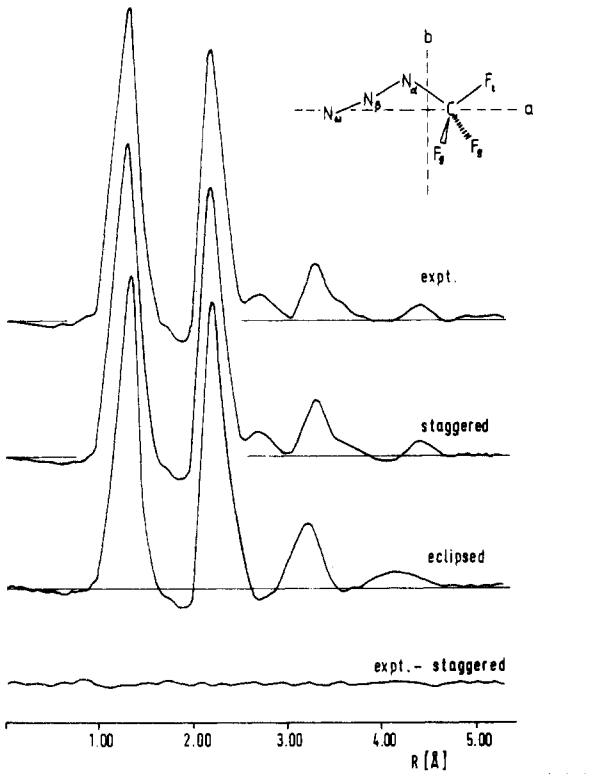

Figure 2. Experimental radial distribution function, theoretical functions for staggered and eclipsed conformations, and the difference curve between experimental and theoretical staggered conformation.

products were nonvolatile and therefore did not interfere with the measurements.

Electron Diffraction. The scattering intensities were recorded with the Balzers gas diffractograph at two camera distances (25 and 50 cm) on Kodak electron image plates (13 × 18 cm). The accelerating voltage was about 60 kV. The sample was cooled to −80 °C, and the nozzle temperature was 15 °C. The camera pressure never exceeded 2×10^{-5} torr during the experiment. Exposure time was 6–9 s for the long and 15–25 s for the short camera distance. The electron wavelength was calibrated with ZnO diffraction patterns. Two plates for each camera distance were analyzed by the usual procedures. Background scattering recorded without gas was subtracted from the 25-cm data. Averaged molecular intensities for both camera distances (s = 1.4–17 and 8–35 Å^{-1}) are presented in Figure 1, and numerical values for the total scattering intensities are available as supplementary data.[10]

Microwave Spectroscopy. The microwave spectrum was recorded at temperatures between −70 and −40 °C at pressures around 10 mtorr and at frequencies between 7 and 25 GHz (X- and K-band) on a standard 100-kHz Stark spectrometer.

CF_3N_3 was initially flowed through the cell, but since the sample proved to be very stable, it was only changed at intervals of several hours.

An initial broad-band sweep in the K-band, applying a 0–20-V ramp voltage at the external sweep connector of the Marconi sweeper, immediately revealed the μ_a R-branch heads typical of a nearly prolate rotor and thus restricted the ranges to be searched.

Table I. Interatomic Distances, Vibrational Amplitudes from Spectroscopic and Electron Diffraction Data, and Vibrational Corrections Δ (Å)

atom pair	r_{ij}	vibrational amplitudes: spectr	vibrational amplitudes: ed[a]	$\Delta = r_a - r_z$
N_β-N_ω	1.12	0.034	0.034[b]	0.0060
N_α-N_β	1.25	0.042	0.042 (4)[c]	0.0004
C-F	1.33	0.045	0.045 (4)[c]	0.0013
C-N_α	1.43	0.053	0.053 (4)[c]	−0.0001
F···F	2.16	0.054	0.056 (3)[c]	0.0009
N_α···F_t	2.18	0.061	0.063 (3)[c]	0.0004
N_α···F_g	2.30	0.063		0.0001
C···N_β	2.23	0.067	0.067[b]	−0.0006
N_α···N_ω	2.36	0.046	0.046[b]	0.0028
N_β···F_g	2.71	0.169	0.174 (26)	−0.0072
C···N_ω	3.27	0.085	0.095 (40)	−0.0003
N_β···F_t	3.31	0.092	0.092[b]	0.0021
N_ω···F_g	3.56	0.229	0.250 (33)	−0.0096
N_ω···F_t	4.42	0.141	0.096 (57)	0.0130

[a] Error limits are 3σ values. [b] Not refined. [c] Ratio constrained to spectroscopic ratio.

Table II. Geometric Parameters (Å and deg) for CF_3N_3 from Electron Diffraction and Combined Electron Diffraction-Microwave Analysis

	$r_\alpha{}^0$ [a]	r_{av} [b]
C-F	1.329 (3)	1.328 (2)
C-N_α	1.427 (5)	1.425 (5)
N_α-N_β	1.250 (7)	1.252 (5)
N_β-N_ω	1.117 (4)	1.118 (3)
$CN_\alpha N_\beta$	111.8 (1.1)	112.4 (0.2)
$N_\alpha N_\beta N_\omega$[c]	175.3 (4.3)	169.6 (3.4)
FCF	108.4 (0.4)	108.7 (0.2)
tilt[d]	4.4 (1.2)	5.8 (0.4)

[a] Results from electron diffraction analysis; error limits are 2σ values and include a possible scale error of 0.1% for bond lengths. [b] Results from combined electron diffraction–microwave analysis; error limits are 2σ values. [c] Bend away from CF_3 group. [d] Tilt of CF_3 group away from N_3 group.

Structure Analysis

A preliminary analysis of the radial distribution function (Figure 2) clearly demonstrates that the CF_3 group is staggered with respect to the N_3 chain. Model calculations for the eclipsed configuration result in very bad agreement with the experimental data in the range $r > 2.5$ Å (see Figure 2). The radial distribution function for the eclipsed configuration was calculated with the final geometric parameters derived for the staggered conformation. Increase of the $CN_\alpha N_\beta$ angle to about 130° improved the fit for the peak at 3.3 Å, but the disagreement for the peaks around 2.7 and 4.5 Å remained. Therefore, in the following analysis the CF_3 group was constrained to the staggered position. However, small torsional deviations (<10°) from this position cannot definitely be excluded.

In the least-squares analysis a diagonal-weight matrix was applied to the intensities and scattering amplitudes, and the phases of Haase[11] were used. The spectroscopic corrections, Δr (Table I), were incorporated into the refinement. For torsional vibrations, the concept of perpendicular (rectilinear)

(10) Supplementary data available (see paragraph at end of paper).

(11) Haase, J. *Z. Naturforsch., A* **1970**, *25A*, 936.

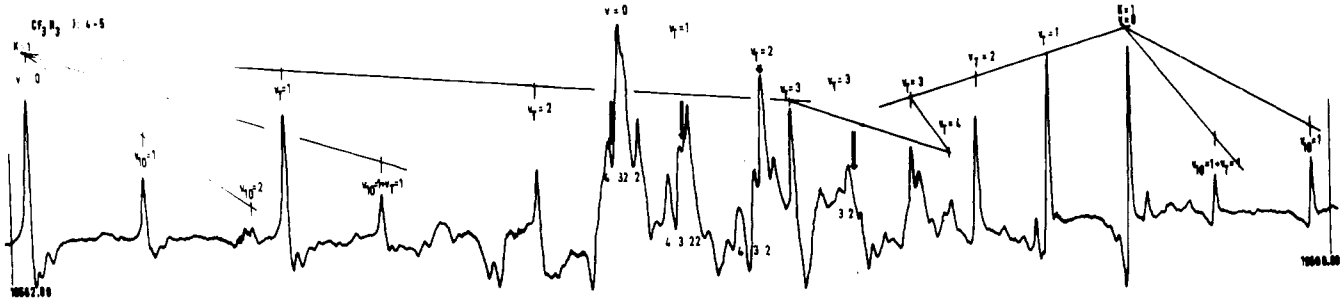

Figure 3. The $J = 4 \rightarrow 5$ rotational transitions at a Stark field of 200 V/cm. Arrows indicate frequencies at which $K_{-1} = 0$ lines appear at higher Stark fields. $v_T = v_{15}$. $v_T = 4$ indicates the center of the A components of the torsionally split $v_T = 4$ state. The $K_{-1} = 1$ lines have not definitively been assigned.

amplitudes results in unrealistically large contributions to these corrections for torsion-independent distances (C–F, F···F, and N···F). Therefore, contributions from the CF_3 torsion, which is a large-amplitude vibration, were neglected for torsion-independent distances.[12] Assuming local C_{3v} symmetry for the CF_3 group with a possible tilt angle between the C_3 axis and the C–N bond, eight geometric parameters (including the $N_\alpha N_\beta N_\omega$ angle) are required for the determination of the structure of CF_3N_3. These parameters were refined simultaneously with six vibrational amplitudes (see Table I). The remaining vibrational amplitudes, which either cause high correlations or are badly determined in the electron diffraction experiment, were constrained to the spectroscopic values, calculated from the force field. This is justified, since the refined amplitudes agree very well with the spectroscopic values. The result from the electron diffraction analysis is included in Tables I and II.

In the final stage of the analysis, structural parameters were fitted to electron diffraction intensities as well as rotational constants.[13] Although the method for calculating $\Delta B^i = B^i_o - B^i_z$ is based on the assumption of small-amplitude vibrations, which certainly does not describe the torsional motion, this approximation has a minor effect on the determination of the geometric parameters. In order to test this effect, structural parameters were calculated by using three different corrections: (1) assuming all vibrations to have small amplitudes (ΔA = 0.39, ΔB = 1.98, and ΔC = −0.78 MHz), (2) disregarding torsion (ΔA = 4.42, ΔB = 1.16, and ΔC = 1.22 MHz), and (3) no corrections at all. The relative weight between electron diffraction and microwave data was adjusted, until the rotational constants were fitted to within 20% of the corrections in cases 1 and 2 and to within 1 MHz in case 3. These calculations demonstrate that the small differences in the rotational constants do not affect the geometric parameters outside the error limits given in Table II.

The results demonstrate the usefulness of the rotational constants for the reduction of the uncertainties in the $CN_\alpha N_\beta$ and the CF_3 tilt angle, which are very sensitive to the asymmetry or, in other words, to $B_z - C_z$.

Normal-Coordinate Analysis

A force field, required for the joint analysis of microwave and electron diffraction data, was derived from the 14 fundamental frequencies determined in a previous study,[6] the torsional frequency, derived from relative intensity measurements of rotational transitions of the excited torsional states, and the centrifugal distortion constant D_{JK}, determined from the rotational spectrum of the ground state.

Valence force constants were refined with the program NCA[14] on the basis of mass-weighted Cartesian coordinates.

(12) Oberhammer, H. *J. Chem. Phys.* **1978**, *69*, 468.
(13) Typke, V.; Dakkhouri, M.; Oberhammer, H. *J. Mol. Struct.* **1978**, *44*, 85.
(14) Christen, D. *J. Mol. Struct.* **1978**, *48*, 101.

Table III. Force Field[a] for CF_3N_3

CF	6.69	CF/CF	1.06
CN	4.84	CF/CN	0.46
$N_\alpha N_\beta$	7.75	CF/FCF (adj)	0.51
$N_\beta N_\omega$	16.88	CF/FCF (opp)	−0.33
FCF	1.82	CN/FCF	−1.00
NCF	1.20	CN/NCF (adj)	0.42
CNN	1.49	CN/NNN	−0.54
NNN	0.67	FCF/FCF	0.23
tors	0.03	FCF/NNN	−0.18
		NNN/tors	−0.07

[a] Stretch in mdyn/Å, stretch/bend in mdyn/rad, and bend in mdyn Å/rad².

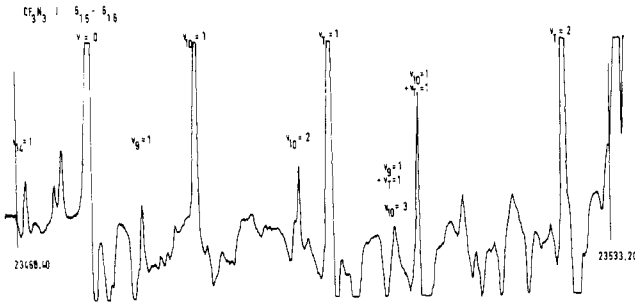

Figure 4. The $J = 5_{15} \rightarrow 6_{16}$ transitions showing several vibrationally excited states at a Stark field of 800 V/cm. $v_T = v_{15}$.

The modified harmonic force field (Table III) looks reasonable, but is, of course, underdetermined.

The mean deviation between measured and calculated frequencies is $\overline{\Delta\nu} = 4$ cm^{-1}.

Rotational Spectrum

The assignment of the band heads in the K-band region to the $J = 4 \rightarrow 5$ (19.62 GHz) and $J = 5 \rightarrow 6$ (23.54 GHz) transitions was straightforward since these band heads appeared very close to the frequencies predicted by the preliminary electron diffraction model ($B + C$ = 3.94 GHz), but the high-resolution recordings did not openly display the characteristic pattern of a nearly prolate (K = −0.989) rotor (see Figure 3). The deviations arise from excited vibrational states—especially the low-lying torsional states—as will be discussed below. The frequencies of all measured transitions and the ensuing rotational constants have been collected in Table IV. The $K_{-1} = 1$ lines stand out quite clearly, though, and recording at different Stark fields permitted the identification of $K_{-1} = 0$ lines that appear only at high fields. Subsequently higher K_{-1} lines were identified, but because many of them are subject to heavy overlapping, some of them could only be measured using a radio-frequency/microwave double-resonance technique (RFMWDR) as described below.

The lowest J lines show signs of quadrupole hyperfine structure, but no attempt was made to resolve and analyze these splittings. Stark measurements on different M compo-

Table IV. Measured Rotational Transitions and Derived Rotational Constants (MHz)

	$v=0$	$v_{15}=1$	$v_{15}=2$	$v_{15}=3$	$v_{15}=4^a$	$v_{10}=1$	$v_{10}=2$	$v_{15}=1, v_{10}=1$	$v_9=1$
$1_{01}2_{02}$	7 845.90	7 848.36	7 851.39	7 854.87	7 858.13	7 851.84	7 857.67	7 853.68	
$2_{12}3_{13}$	11 738.22	11 750.70	11 764.13	11 778.62		11 743.79	11 749.23	11 755.80	
$2_{02}3_{03}$	11 768.73	11 772.52	11 777.05	11 782.32	11 787.38	11 777.53		11 780.40	
$2_{21}3_{22}$	11 768.73	11 772.33	11 776.69	11 781.82		11 777.72		11 780.28	
$2_{20}3_{21}$	11 768.93	11 772.49	11 776.69	11 781.82		11 778.00		11 780.51	
$2_{11}3_{12}$	11 799.67	11 794.40	11 789.80	11 785.77				11 805.19	
$4_{14}5_{15}$	19 563.32	19 584.34	19 606.66	19 630.92		19 572.60	19 581.52	19 592.76	
$4_{41}5_{42}$ / $4_{40}5_{41}$	19 612.98	16 618.70	19 625.77	19 633.66		19 627.90		19 632.07	
$4_{04}5_{05}$	19 613.36	19 620.17	19 627.90	19 637.11	19 646.89	19 627.75	19 641.95	19 633.17	
$4_{32}5_{33}$ / $4_{31}5_{32}$	19 614.09	19 619.84	19 626.93	19 635.37		19 629.06	19 643.67	19 633.17	
$4_{23}5_{24}$	19 614.28	19 620.17	19 627.75	19 636.38		19 629.06	19 643.67	19 633.58	
$4_{22}5_{23}$	19 615.96	19 621.02	19 627.90	19 636.38			19 646.29	19 634.74	
$4_{13}5_{14}$	19 665.79	19 657.02	19 649.58	19 642.92		19 686.00	19 706.00	19 675.23	
$5_{15}6_{16}$	23 475.69	23 500.96	23 527.92	23 557.02		23 486.68	23 497.42	23 510.98	23 480.85
$5_{51}6_{52}$ / $5_{50}6_{51}$	23 534.01	23 540.81	23 549.30			23 551.87			
$5_{05}6_{06}$	23 534.97	23 543.71	23 553.54	23 564.72		23 552.18	23 568.80		
$5_{42}6_{43}$ / $5_{41}6_{42}$	23 535.65	23 542.48	23 551.08	23 560.39		23 553.51			
$5_{24}6_{25}$	23 536.98	23 544.36	23 553.06	23 563.73		23 554.88		23 560.39	
$5_{33}6_{34}$ / $5_{32}6_{33}$	23 537.01	23 543.71	23 552.40	23 562.22		23 554.88			
$5_{23}6_{24}$	23 540.01	23 545.76	23 553.54	23 563.73		23 558.48		23 562.22	
$5_{14}6_{15}$	23 598.62	23 588.29	23 579.39	23 571.50		23 662.84	23 646.77	23 609.94	23 607.58
A^b	5544	5631.5	5722.4	5817.2	5880.5	5517.5	5490	5600	5526.5
B	1971.750 (4)	1969.374 (6)	1967.121 (6)	1964.924 (7)	3929.1[c]	1974.335 (6)	1976.896 (5)	1971.679 (6)	1967.30
C	1951.260 (4)	1954.825 (6)	1958.544 (6)	1962.519 (7)		1951.648 (6)	1952.002 (5)	1955.188 (6)	1956.74
$D_{JK}{}^d$	0.0142 (1)	0.0150 (2)	0.0158 (2)	0.0220 (31)		0.0143 (2)	0.0141 (5)	0.0148 (3)	0[e]

[a] A species. [b] Fixed to value determined from structural model and harmonic effects. [c] $B + C$. [d] kHz. [e] Assumed.

nents of the transitions $4_{14} \rightarrow 5_{15}$, $4_{13} \rightarrow 5_{14}$, $5_{15} \rightarrow 6_{16}$, and $5_{14} \rightarrow 6_{15}$ (calibrating the field against the OCS shifts and using Muenter's value for its dipole moment[15]) yielded a dipole moment in the a direction of $\mu_a = 1.15$ (10) D.

To understand the microwave spectrum in detail, especially the many lines between the two $K_{-1} = 1$ transitions, it is necessary to consider the possible molecular vibrations. In an earlier study,[6] the vibrational spectra were investigated and 14 of the 15 fundamentals identified. The missing one, the torsion of the CF_3 group, was predicted to lie below 90 cm^{-1} but could not experimentally be observed.

Figure 4 shows the $5_{15} \rightarrow 6_{16}$ transition in a highly amplified recording. From the characteristic Stark patterns it is possible to identify all of the obvious lines with the same transition, only in different vibrational states. The very intense progression to higher frequency must be assigned to the torsion, and relative intensity measurements using the Wilson–Nesbitt method[16] yield an energy above the ground state of 47 (3) cm^{-1} for the first excited torsional state and thus for the torsional frequency.

To test the reliability of this method, the energies of excited states of other vibrations were determined and compared to the fundamental frequencies determined from the IR and Raman spectra (in parentheses): ν_{10} 177 (179), ν_9 409 (402), ν_{14} 459 (450), $\nu_{10} + \nu_{15}$ 221 cm^{-1} comprised of ν_{10} 174 and ν_{15} 47 cm^{-1}.

The reliability of the method obviously decreases with increasing frequency (decreasing intensity), and the method fails for transitions falling between the two $K_{-1} = 1$ lines because of serious overlapping of lines and Stark components.

Examination of the $5_{14} \rightarrow 6_{15}$ transitions to determine their relative intensities revealed that the ν_{15} progression extends toward lower frequencies, and thus the frequency difference between the $K_{-1} = 1$ lines decreases with increasing excitation of ν_{15}. This effect is not observed with the other excited states (notably ν_{10}). The frequency difference between the $K_{-1} = 1$ lines directly determines $B - C$, and thus the observed trend indicates an increase in symmetry in the ν_{15} progression.

In order to explain this trend, it must be noted that a structural model having the C_3 axis of the CF_3 group collinear with the C–N bond only produces a $B - C$ value of 1–2 MHz. To reproduce the observed $B - C$ value for the ground state (20.5 MHz), it is necessary to assume a tilt angle of ~5°.

Consequently, one could propose that the effect of higher torsional excitation is the removal of the tilt of the CF_3 group. In that case one would expect higher torsional states to have $B - C$ values between 1 and 2 MHz.

On the other hand, if one realizes that most of the molecular mass is concentrated in the trifluoromethyl group, it is possible to visualize the light "frame" rotating about the heavy "top", and higher excitation would lead to an effective symmetric-top molecule with the excited energy levels lying well above the barrier to the torsional motion. In that case, however, as the energy levels approach the top of the barrier, tunneling through the threefold barrier would cause the rotational lines to split into nondegenerate A and doubly degenerate E components.

Unfortunately, this splitting is expected to take place at the frequency where the center of the rotational transitions of the excited torsional states have "turned back" (see Figure 3) into the upper $K_{-1} = 1$ lines of the lower torsional states, and thus it is impossible to clearly distinguish the weaker lines of the higher excited states.

It was hoped that double-resonance experiments (RFMWDR) could circumvent this problem.[17] RFMWDR techniques were used to identify and measure the $J = 5 \rightarrow 6$, $K_{-1} = 2$ transitions of the molecule in its ground as well as its first excited torsional state, with a pump frequency of 3.1 MHz, which happens to be the asymmetry splitting of the $J = 5$ levels for the ground state and the splitting of the $J = 6$

(15) Muenter, J. S. *J. Chem. Phys.* **1968**, *48*, 4544.
(16) Nesbitt, A. S., Jr.; Wilson, E. B., Jr. *Rev. Sci. Instrum.* **1963**, *34*, 901.
(17) Wodarczyk, F. J.; Wilson, E. B., Jr. *J. Mol. Spectrosc.* **1971**, *37*, 445.

Table V. Principal Geometric Parameters (Å and deg) of Some Azides, XN_3, Studied in the Gas Phase

	HN_3[b]	CH_3N_3[c]	Me_3SiN_3[d]	ClN_3[e]	NCN_3[f]	CF_3N_3[g]
$X-N_\alpha$	1.015 (15)	1.468 (5)	1.734 (7)	1.745 (5)	1.355 (2)	1.425 (5)
$N_\alpha-N_\beta$	1.243 (5)	1.216 (4)	1.198 (8)	1.252 (10)	1.261 (2)	1.252 (5)
$N_\beta-N_\omega$	1.134 (2)	1.130 (5)	1.150 (11)	1.133 (10)	1.121 (2)	1.118 (3)
$XN_\alpha N_\beta$	108.8 (4.0)	116.8 (0.3)	128.0 (1.6)	108.7 (0.5)	114.5 (0.2)	112.4 (0.2)
$N_\alpha N_\beta N_\omega$	171.3 (5.0)	180[h]	180[h]	171.9 (0.5)	169.2 (1.6)	169.6 (3.4)
τ[a]		35.0 (7.0)	24.0 (5.0)			0.0

[a] Torsional angle of group X around X–N bond. $\tau = 0°$ corresponds to staggered position. [b] r_s values; ref 18. [c] r_a values; ref 7b. [d] r_a values; ref 19. [e] r_s/r_0 values; ref 20. [f] r_α values; ref 21. [g] r_{av} values; this study. [h] Estimated value.

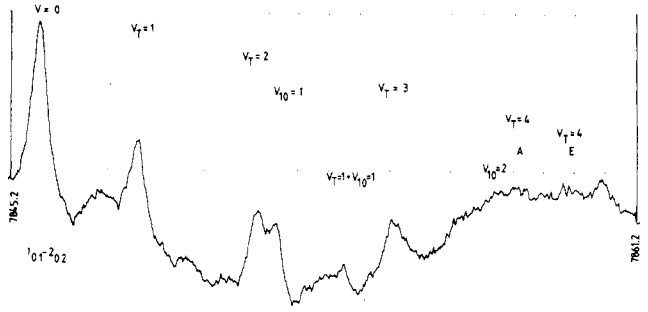

Figure 5. The $J = 1_{01} \rightarrow 2_{02}$ transitions at a Stark field of 800 V/cm. Marker spacing is 0.8 MHz. The assignment of $v_T = 4$ is speculative, although other J candidates for the A components have been located.

levels for the first excited torsional state. With a pump frequency of 6.15 MHz (the ground-state splitting of the $J = 6$ levels) only the ground-state transitions are observed.

It was also possible to observe the $K_{-1} = 1$ lines in RFMWDR ($J = 5 \rightarrow 6$) for the ground state ($\nu_P = 307.0$ MHz) and the first ($\nu_P = 218.4$ MHz), the second ($\nu_P = 128.7$ MHz), and, barely, the third excited torsional states ($\nu_P = 36.1$ MHz).

The weakness of the third excited torsional state transitions extinguished the hope of finding the $v_{15} = 4$ lines by using the DR technique, which would otherwise have overcome the problem of overlapping.

Fortunately, however, the $J = 1 \rightarrow 2$ transitions around 7.9 GHz (Figure 5), modulated at a Stark field of 800 V/cm, only show the $K_{-1} = 0$ transitions and thus provide a somewhat clearer picture. It looks as though the $v_{15} = 3$ transition is somewhat broadened compared to the $v_{15} = 0$, 1, and 2 transitons, and the $v_{15} = 4$ transition is possibly split into two components, indicating a torsional level approaching the top of the barrier.

The assumption of a purely sinusoidal potential allows a determination of the barrier heights from the torsional force constant, known from the normal-coordinate analysis

$$\text{force constant} = \frac{\partial^2 V}{\partial \alpha^2} = \frac{\partial^2}{\partial \alpha^2}\left[\frac{V_3}{2}(1 - \cos(3\alpha))\right]$$

$$\text{at } \alpha = 0 = 9V_3/2$$

or 0.03 mdyn Å^2 = 4.35 kcal/mol = $9V_3/2$ and $V_3 = 0.97$ kcal/mol.

Thus, the $v_{15} = 4$ state with an energy of 0.675 kcal is in fact quite close to the top of the barrier, especially since the addition of a few percent V_6 potential would somewhat lower the value of V_3. It seems, although the evidence is sparse, that the decrease in $B - C$ on excitation of v_{15} is due to the hindered internal rotation of the trifluoromethyl group.

Discussion

The most significant features of the CF_3N_3 structure are the bond lengths, the nonlinearity of the N_3 group, and the torsion and tilt angle of the CF_3 group with respect to the N_3 group. These features are discussed in the following paragraphs.

Bond Lengths. The above results clearly demonstrate that in CF_3N_3 the $N_\beta-N_\omega$ bond is significantly shorter than the $N_\beta-N_\alpha$ bond. This can be attributed to the electron-withdrawing effect of the CF_3 group. A comparison of the MN_3 series (M = alkali metal, $(CH_3)_3Si$, H, Cl, CF_3) shows that if M is of very low electronegativity, as for example in the alkali metals, we have an ionic $M^+N_3^-$ structure (I) with two

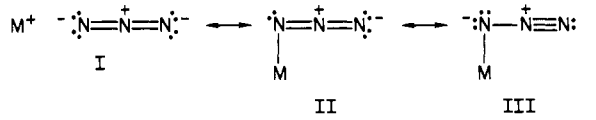

degenerate N–N bonds of 1.16 Å each. With increasing electronegativity of M, the M–N bond becomes more covalent and the contribution from resonance structure III increases, due to the electron-withdrawing effect of M. This causes an increase in the bond length difference between $N_\beta-N_\omega$ and $N_\beta-N_\alpha$ (see Table V). A comparison of the C–N bond lengths in CH_3N_3 and CF_3N_3 also shows the expected effect.[9] Replacement of the CH_3 by the CF_3 group results in bond shortening if the groups are bonded to electronegative atoms or groups. Hence the C–N bond in CF_3N_3 (1.425 Å) is significantly shorter than that in CH_3N_3 (1.468 Å).

Torsional Angle of the CX_3 Group. In general, methyl or trifluoromethyl groups prefer the staggered position with respect to single bonds but prefer an eclipsed position with respect to double bonds. Representative examples in the case of C=C double bonds are $CX_3CH=CH_2$[22] and *trans*-$CX_3CH=CHCX_3$.[23,24] Only strong steric repulsions can force CF_3 groups to abandon the eclipsed position, such as in *cis*-$CF_3CH=CHCF_3$.[24] Only one example is known for N=N double bonds: *trans*-$CX_3N=NCX_3$,[24-26] where the CX_3 groups again eclipse the N=N double bond and stagger the N lone pair. In CF_3N_3 the CF_3 group occupies a staggered position with respect to the N_3 group as shown by IV, and this

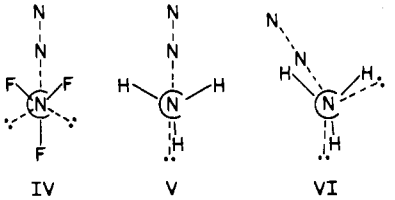

indicates a significant contribution from resonance sttructure III. For this structure, configuration IV minimizes the re-

(18) Winnewisser, B. P. *J. Mol. Spectrosc.* **1980**, *82*, 220.
(19) Dakkhouri, M.; Oberhammer, H. *Z. Naturforsch., A* **1972**, *27A*, 1331.
(20) Cook, R. L.; Gerry, M. C. L. *J. Chem. Phys.* **1970**, *53*, 2525.
(21) Almenningen, A.; Bak, B.; Jansen, P.; Strand, T. G. *Acta Chem. Scand.* **1973**, *27*, 1531.
(22) Tokue, J.; Fukuyama, T.; Kuchitsu, K. *J. Mol. Struct.* **1973**, *17*, 207.
(23) Almenningen, A.; Anfinsen, I. M.; Haaland, A. *Acta Chem. Scand.* **1970**, *24*, 43.
(24) Bürger, H.; Pawelke, G.; Oberhammer, H. *J. Mol. Struct.* **1982**, *84*, 49.
(25) Chiang, C. H.; Porter, R. F.; Bauer, S. H. *J. Am. Chem. Soc.* **1970**, *92*, 5315.
(26) Almenningen, A.; Anfinsen, I. M.; Haaland, A. *Acta Chem. Scand.* **1970**, *24*, 1230.

pulsion between the fluorine free valence electrons and the *two* sterically active free electron pairs on the N_α atom (indicated by broken lines in IV). In contrast to CF_3N_3, the CH_3 group in CH_3N_3 appears to be in an intermediate position between eclipsed and staggered,[7b] (25 ± 7° from the eclipsed position), which may be explained in the following manner: resonance structure II should result in a staggered configuration (V) and resonance structure III in an eclipsed (VI) configuration. Since, as discussed above, the bond lengths indicate that structure II contributes more strongly to the structure of CH_3N_3 than to that of CF_3N_3, the observation of an intermediate torsional angle is not surprising.

Linearity of the N_3 Group and CF_3 Tilt Angle. In CF_3N_3 the N_3 group is slightly (10°) bent away from the CF_3 group, and the CF_3 group is tilted away from the N_3 group by 5.8°. This is readily explained by the repulsion between the fluorine free valence electron pairs and the π-bond electron system of the N_3 group. A comparison of these values with those in CH_3N_3 would be most interesting, but unfortunately no experimental values are presently available for CH_3N_3. It is interesting to note that the angles of the N_3 group found for HN_3, ClN_3, NCN_3, and CF_3N_3 are all very similar. However, it should be kept in mind that most of these values carry rather large uncertainties.

Torsional Effects on the Structure. The present data for the excited torsional states do not allow a determination of the structural changes upon excitation of ν_{15}. It is clear from model calculations, however, that several parameters must change their value in order to reproduce the rotational constants of the excited states. Thus heavy relaxation, not only in the trifluoromethyl group but also in the tilt and the $CN_\alpha N_\beta$ angle, is assumed to take place.

Acknowledgment. We are grateful to Dr. G. Pawelke for providing a sample of CF_3N_3 for the RFMWDR measurements. D.C. and H.O. acknowledge financial support by the Fonds der Chemie. K.O.C. and C.J.S. thank the Office of Naval Research and the U.S. Army Research Office for financial support.

Registry No. CF_3N_3, 3802-95-7.

Supplementary Material Available: Listings of total electron diffraction intensities for two camera distances (50 and 25 cm) for two sets of plates (2 pages). Ordering information is given on any current masthead page.

Contribution from the Department of Inorganic Chemistry, Charles University, 12840 Prague, Czechoslovakia

Rhodium(I) Carbonyl Complexes of (Diphenylphosphino)acetic Acid

A. JEGOROV, B. KRATOCHVÍL, V. LANGER,[1] and J. PODLAHOVÁ*

Received March 6, 1984

Rhodium(I) and (diphenylphosphino)acetic acid (HA) form trans square-planar complexes $Rh(CO)X(HA)_2$ (X = Cl, Br, I) and Rh(CO)A(HA), in which HA acts as a P-monodentate ligand and A^- as a P,O-chelating ligand. All the complexes are fairly reactive and readily undergo oxidative-addition reactions. In the solid state, the latter complex forms several crystalline modifications. The X-ray crystal structure determination of α-carbonyl((diphenylphosphino)acetato-*P,O*)-((diphenylphosphino)acetic acid-*P*)rhodium(I), α-Rh(CO)A(HA), demonstrated a distorted square-planar arrangement around rhodium with Rh–C = 1.773 (11) Å, Rh–P(monodentate) = 2.346 (2) Å, Rh–P(chelating) = 2.302 (2) Å, Rh–O = 2.064 (6) Å, and P–Rh–P = 170.8 (1)°. The distortion due to the chelating A^- anion renders the carbon monoxide sterically more accessible than in complexes of monodentate phosphines. There is a short Rh–H interaction of 2.80 (7) Å with a phenyl ortho hydrogen atom of the HA ligand, which forces the rhodium atom 0.03 Å out of the plane of the donor atoms. Two formula units of the complex are hydrogen bonded, forming a centrosymmetrical dimer. The complex crystallizes in space group $P\bar{1}$ with a = 9.783 (4) Å, b = 11.702 (6) Å, c = 13.120 (6) Å, α = 76.87 (4)°, β = 81.21 (4)°, γ = 71.77 (4)°, and Z = 2. The structure was refined anisotropically to R = 0.053 on the basis of 2367 unique reflections.

Introduction

The investigation of functionalized phosphines has recently received a great deal of attention[2] for both theoretical and practical reasons. The unusual combination of hard and soft donor atoms in these ligands leads to interesting structural types and/or reactivity of the complexes, which is potentially useful, e.g. in homogeneous catalysis. In our laboratory, phosphinoacetic acids of the types $(C_6H_5)_{3-n}P(CH_2CO_2H)_n$, n = 1–3, and $(C_6H_5)_{2-m}(HO_2CCH_2)_mPCH_2CH_2P(C_6H_5)_{2-m}(CH_2CO_2H)_m$, m = 1, 2, were synthesized and their complexes with a number of metal ions were studied.[3] Depending on the metal ion, acidity, and solvent, the ligands are capable of coordinating as P–, O–, PP–, PO–, and POO– donors. This work deals with rhodium(I) carbonyl complexes of (diphenylphosphino)acetic acid.

Experimental Section

Materials. The synthesis of HA has been described.[4] The $[Rh(CO)_2Cl]_2$ complex was prepared[5] from hydrated rhodium trichloride (Safina). Known methods were employed for the preparation of $[Rh(CO)_2X]_2$ (X = Br, I;[6] SCN, NO_3, CH_3CO_2, $^1/_2$ SO_4;[7] N_3, NCO[8]) and for $Rh(CO)_2$acac.[9] Other chemicals were of CP grade and were purified by using standard methods where necessary.

Methods. The preparative work and manipulations with solutions were carried out under nitrogen. IR spectra were measured in solution

(1) Institute of Macromolecular Chemistry, Czechoslovak Academy of Sciences, Prague, Czechoslovakia.
(2) Braunstein, P.; Matt, D.; Dusausoy, Y.; Fischer, J.; Mitschler, A.; Ricard, L. *J. Am. Chem. Soc.* **1981**, *103*, 5115 and references therein.
(3) Nosková, D.; Podlahová, J. *Polyhedron* **1983**, *2*, 349 and references therein.
(4) Jarolím, T.; Podlahová, J. *J. Inorg. Nucl. Chem.* **1976**, *38*, 125.
(5) McCleverty, J. A.; Wilkinson, G. *Inorg. Synth.* **1966**, *8*, 211.
(6) Johnson, B. F. G.; Lewis, J.; Robinson, P. W.; Miller J. R. *J. Chem. Soc. A* **1969**, 2693.
(7) Lawson, D. N.; Wilkinson, G. *J. Chem. Soc.* **1965**, 1900.
(8) Busetto, L.; Palazzi, A.; Ros, R. *Inorg. Chem.* **1970**, *9*, 2792.
(9) Varshavsky, Yu. S.; Cherkasova, T. G. *Zh. Neorg. Khim.* **1967**, *12*, 1709.

0020-1669/84/1323-4288$01.50/0